# Simulation of Texture Development in a Deep Drawing Process

V. Schulze[1], A. Bertram[1], T. Böhlke[2], and A. Krawietz[3]

[1] Institut für Mechanik, Otto-von-Guericke-Universität Magdeburg
[2] Institut für Technische Mechanik, Universität Karlsruhe (TH)
[3] Technische Fachhochschule Berlin

**Abstract.** In this paper the effect of the texture development during the deep drawing of a ferritic steel is studied with a reduced crystal plasticity model. This model has been developed for the application in the forming and springback simulation for industrial applications. Based on a specific optimisation scheme, the number of crystals used at each integration point of the finite elements is reduced to less than 100. Even with such a low number of crystals, it is possible to predict the qualitative development of the texture during the deep drawing process.

## 1 Introduction

In the development of tools for deep drawing processes, the application of finite element based simulations has become a standard procedure. While the prediction of the strain distribution can be performed with significant precision using conventional phenomenological material models, these models lack to predict the development of the anisotropy of the material during the metal forming operation. The latter is of high interest for the prediction of stresses in the material. With this information, the accuracy of the springback simulation as well as the prediction of the failure of the material can be improved. In this study, a micro-mechanical approach is used to model the material behaviour. Typical examples of phenomenological material models used in commercial finite element codes are the Hill-48 model implemented in PamStamp and the similar Barlat-89 model in LS-Dyna (Hallquist 1998; Hill 1948; Barlat and Lian 1989). These models are able to approximate the anisotropy of the yield locus by three parameters ($r$-values) that can be identified by tension tests in three directions. These relatively simple models have been extended to more sophisticated models, e.g., by Barlat et al. (2005). All these models have the assumption in common that the anisotropy of the material remains constant during the deformation process.

Conventional ferritic steels consist of agglomerates of body-centred cubic crystals. While the deformation of these crystals can be modelled fairly easily, the complex macroscopic behaviour is the result of the orientation distribution, morphology, and interaction of the grains. Therefore, such a micro-mechanical material model has the advantage that the development of the material behaviour is much less restricted compared to phenomenological models. However, the improvement in the material

description definitely requires an increased computational effort, which depends on the material modelling of the crystals, the type of the micro-macro-transition, and the number of crystals taken into account.

There are many approaches that are used for the micro-macro-transition, such as the relaxed constraint (RC) models (Honneff and Mecking 1978), self-consistent (SC) models (Kröner 1961), and finite element models, in which a representative volume element is used in the homogenisation schemes (Bronkhorst et al. 1992; Böhlke et al. 2007). A major drawback of these more detailed approaches is that they are either modelled for specific load cases (RC-models) or lead to a large additional computational effort compared with the rather simple Taylor model. Consequently, the latter methods are typically limited to very detailed simulations of small material regions. A special aspect of crystal plasticity models for anisotropic materials is the need to approximate the initial texture of the material under consideration. The field of the texture approximation has been the topic of intensive studies itself (see, e.g., Böhlke et al. 2006b; Risy 2007; Böhlke et al. 2008). The number of crystals needed for this approximations has an important impact on the computational effort. In many cases it is possible to approximate a measured texture by a group of texture components, which can be described by a mean orientation and a corresponding scatter parameter. Many studies use special techniques to calibrate these components by the measured texture (see, e.g., Toth and Van Houtte 1992; Böhlke et al. 2006a).

In order to improve the accuracy of finite element simulations of forming operations and springback, we use a crystal plasticity model for bcc crystals, which has been implemented in a user subroutine in the finite element code LS-Dyna (Hallquist 1998). The rate-independent crystal plasticity model uses the pencil glide assumption to reduce the computational effort on the micro scale. The homogenization is based on the Taylor assumption. Special emphasis is given to an approximation of the crystallographic texture by a low number of crystal orientations without overestimating the mechanical anisotropy. Therefore, the number of crystals is minimized by a special approximation procedure in combination with an isotropic background model. The results from this model are compared with experimental measurements as well as with the results of the standard Barlat-89 model (Barlat and Lian 1989).

**Notation.** Throughout the text, a direct tensor notation is preferred. The scalar product and the dyadic product are denoted by $\boldsymbol{A} \cdot \boldsymbol{B} = \mathrm{tr}(\boldsymbol{A}^{\mathrm{T}}\boldsymbol{B})$ and $\boldsymbol{A} \otimes \boldsymbol{B}$, respectively. A linear mapping of 2nd-order tensors by means of a forth-order tensor $\mathbf{C}$ is written as $\boldsymbol{A} = \mathbf{C}[\boldsymbol{B}]$. Traceless tensors (deviators) are designated by a prime, e.g., $\boldsymbol{A}'$. A superimposed bar indicates that the quantity corresponds to the macroscale.

## 2 Constitutive Equations

In the following the multiplicative decomposition of the deformation gradient $\boldsymbol{F} = \boldsymbol{F}_e\boldsymbol{F}_p$ into an elastic part $\boldsymbol{F}_e$ and a plastic part $\boldsymbol{F}_p$ will be used, see e.g., Krawietz 1986; Bertram 1999, 2008). It is further assumed that a linear relation between a generalized stress and a corresponding generalized strain measure can be used for the formulation of the elastic law, since the elastic strains are small. For this study, the St.



Venant-Kirchhoff law formulated in terms of quantities with respect to the undistorted configuration

$$\boldsymbol{S}_e = \mathbf{C}[\boldsymbol{E}_e] \text{ with } \boldsymbol{S}_e = \det(\boldsymbol{F}_e)\,\boldsymbol{F}_e^{-1}\,\boldsymbol{\sigma}\,\boldsymbol{F}_e^{-\mathrm{T}} \tag{1}$$

the 2nd Piola-Kirchhoff stress tensor, $\boldsymbol{\sigma}$ the Cauchy stress tensor, $\boldsymbol{E}_e = (\boldsymbol{C}_e - \boldsymbol{I})/2$ Green's strain tensor, and $\boldsymbol{C}_e = \boldsymbol{F}_e^{\mathrm{T}}\boldsymbol{F}_e$ the right (elastic) Cauchy-Green tensor. For the modeling of the plastic flow, an evolution equation for the plastic part of the deformation gradient is used

$$\dot{\boldsymbol{F}}_p\boldsymbol{F}_p^{-1} = \sum_{\alpha\in\mathrm{A}}^{N} \dot{\gamma}_\alpha \boldsymbol{d}_\alpha \otimes \boldsymbol{n}_\alpha \tag{2}$$

with the slip rate $\dot{\gamma}_\alpha$, the slip direction $\boldsymbol{d}_\alpha$, and the slip plane normal $\boldsymbol{n}_\alpha$ of the slip system $\alpha$. $A$ denotes the set of active slip systems. $N$ is the total number of slip systems. The yield condition in each glide system is given by a scalar equation depending on the weighted shear stress $\tau_\alpha$ and the critical resolved shear stress $\tau_\alpha^C$ after Schmid

$$\phi_\alpha\left(\tau_\alpha, \tau_\alpha^C\right) = |\tau_\alpha| - \tau_\alpha^C = 0$$

The weighted shear stress $\tau_\alpha$ is determined by the projection of the weighted Mandel stress tensor $\boldsymbol{Z}_e = \boldsymbol{C}_e\boldsymbol{S}_e/\rho_0$ into the slip system $\tau_\alpha = \boldsymbol{Z}_e \cdot \boldsymbol{d}_\alpha \otimes \boldsymbol{n}_\alpha$ with $\rho_0$ being the mass density in the reference placement.

Ferritic steels consists of body-centred cubic crystals (bcc). The primary glide systems of these crystals are the {110}<111>, {112}<111>, and {123}<111> systems. In a conventional rate-independent crystal model, all these glide systems have to be tested for admissible combinations that satisfy the yield condition and the consistency condition. A systematic testing sequence would be cumbersome. In the context of pencil glide for given slip directions $\boldsymbol{d}_\alpha$ corresponding to the lattice directions <111>, only the slip plane normals $\boldsymbol{n}_\alpha$ have to be determined. For given stress state

$$\boldsymbol{n}_\alpha = \frac{1}{\mu}\boldsymbol{s}_\alpha,\quad \boldsymbol{s}_\alpha = (\boldsymbol{I} - \boldsymbol{d}_\alpha \otimes \boldsymbol{d}_\alpha)\boldsymbol{Z}_e^{\mathrm{T}}\boldsymbol{d}_\alpha,\quad \mu = \|\boldsymbol{s}_\alpha\| \tag{3}$$

determines a shear vector for each slip direction $\boldsymbol{d}_\alpha$ (Schulze et al. 2007). Since the vector $\boldsymbol{s}_\alpha$ is orthogonal to the glide direction $\boldsymbol{d}_\alpha$, one derives the result

$$\tau_\alpha = \boldsymbol{s}_\alpha \cdot \boldsymbol{n}_\alpha = \|\boldsymbol{s}_\alpha\| = \mu.$$

The hardening is modelled by a phenomenological approach based on an accumulated slip in each slip system. We assume that the critical weighted shear stress $\tau_\alpha^C$ depends on a hardening parameter $\xi_\alpha$, defined by

$$\dot{\xi}_\alpha = (1-q)\dot{\gamma}_\alpha + q\sum_\beta \dot{\gamma}_\beta\,, \tag{4}$$

where $q$ is the ratio of self and latent hardening. The hardening is modelled by the ansatz of Swift

$$\tau_\alpha^C = A_1\left(1 + A_2\xi_n\right)^n. \tag{5}$$

Since the model is meant for industrial applications, the micro-macro transition is performed by the Taylor model (Taylor 1938). The Taylor model typically overestimates the anisotropy of a material. This drawback of this model is even increased, if only a small number of discrete crystals is used. Therefore, an isotropic background model is needed. Here an isotropic von Mises plasticity model with fictitious volume fraction is used (hybrid model) in order to model the grey texture.

## 3 Model Identification and Finite Element Simulation

The material DX53D+Z used in this study is a mild ferritic deep drawing steel. The identification of the crystal plasticity model is performed in two stages. In the first step, the initial texture of the material is approximated. With the fixed initial orientation of the crystals in the model, the elastic and plastic constants are approximated using macroscopic measurements in a second step. Details concerning the parameter identification are given in Schulze et al. (2007). The approximation of the texture is based on a mixed integer quadratic approximation scheme using sharp components with the same scatter to approximate a given texture (Böhlke et al. 2006a). The advantage of this method is that it can be applied to arbitrary crystal and texture classes, the existence of an error bound for the approximation, and the user-independence of the approximation results.

With this approximation, the initial orientation of the crystals as well as their respective volume fraction can be determined in one optimisation procedure. For the verification of the material model, the deep drawing of a circular cup is performed. Subsequent to this process, the cups are cut into slices or rings, and these rings are opened so that the springback of the part can be evaluated (Rohleder 2002). Furthermore, samples are taken from the cups in order to determine the texture after the deformation. The surface texture of the material is measured by conventional X-rays.

**Table 1.** Material parameters of DX53 D+Z

| | $E$ in GPa | $G$ in GPa | $\nu$ | $q$ | $A_1$ GPa | $A_2$ | $n$ | $\xi_0$ | $v_{iso}$ |
|---|---|---|---|---|---|---|---|---|---|
| A16M | 114.88 | 94.99 | 0.3302 | 1.4 | 0.0299 | 410.090 | 0.275 | 0.0330500 | 0.56 |
| A32M | 114.35 | 94.82 | 0.3320 | 1.4 | 0.0292 | 409.970 | 0.270 | 0.0330500 | 0.54 |
| A48M | 111.60 | 95.00 | 0.3415 | 1.4 | 0.0271 | 400.147 | 0.278 | 0.0326575 | 0.54 |
| A64M | 113.97 | 94.71 | 0.3304 | 1.4 | 0.0291 | 414.920 | 0.270 | 0.0330500 | 0.52 |
| A80M | 114.30 | 94.81 | 0.3307 | 1.4 | 0.0292 | 409.960 | 0.270 | 0.0330400 | 0.52 |
| A96M | 113.75 | 94.63 | 0.3334 | 1.4 | 0.0292 | 409.940 | 0.270 | 0.0330400 | 0.50 |



The simulation of the deep drawing process uses the meshed CAD-geometry of the tools. The tool elements are rigid bodies and used to simulate the contact between the tool and the blank. The blank is modelled by under-integrated Belytschko-Lin-Tsay elements (Hallquist 1998), which are routinely used in industrial computations. In the simulation, a friction coefficient of $\mu = 0{,}075$ is used. This value has been determined in separate measurements. The penalty parameter is equal to the suggested value for LS-Dyna (Hallquist 1998). The material parameters are given in Tab. 1. Details of the identification scheme can be found in (Schulze et al. 2007).

## 4 Results and Discussion

The results of the strain distribution in the rolling direction for DX53D+Z are given in Figs. 1 and 2. The strain cuts show a distinct increase in the accuracy of the prediction of the major and minor strains compared with the reference model.

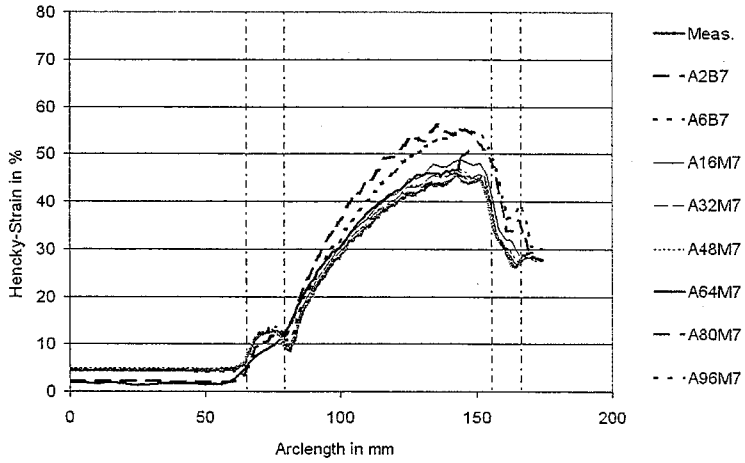


**Fig. 1.** Major strain in rolling direction

Considering the prediction of the earing, the result is improved by the application of the crystal plasticity model in combination with the von Mises model for the background. Only the model with 16 crystals is unable to reproduce the shape of the earing after the deformation (Fig. 3-4). For the models with 32 or more crystals, the result is in good agreement with the measurements. The mean error of the flange draw-in is reduced from more than 3.3mm in the reference model to less than 1.6mm in the crystal models. The earing height predicted by the Barlat models is in the range of more than 10mm while it is less than 4 mm with the hybrid models with more than 32 crystals, and, therefore, within the range of the measurements (3.6mm ± 0.7mm). The

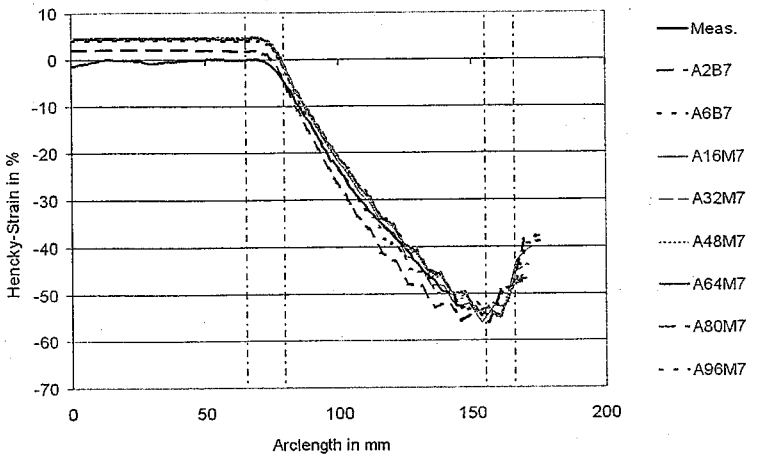


**Fig. 2.** Minor strain in rolling direction

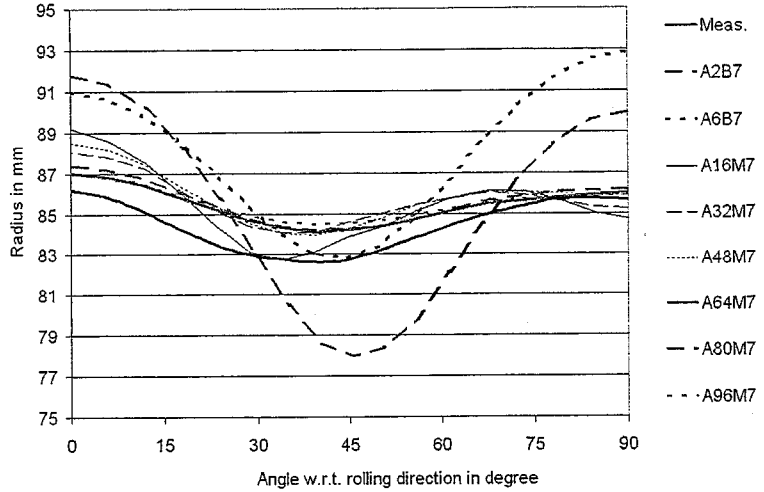


**Fig. 3.** Earing profile for models with isotropic background

measurements of the texture of DX53 after the deep drawing shows that the fibre structure of the texture has been transformed into a dominant component. Due to symmetry reasons, this component appears twice in the Euler space representation. The odf-plots are given in Fig. 5(a) in cuts in the $\varphi_2$-direction.



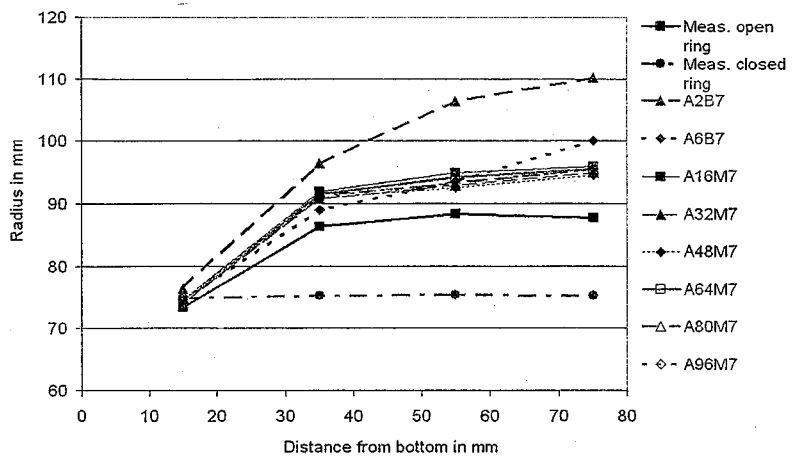


**Fig. 4.** Springback results: Barlat model (7 IP), crystal model with the isotropic von Mises component (7 IP)

The simulation clearly shows the development of the crystallite orientation. The results of this development are given in Fig. 5-6. The single crystals have been approximated with single components by a half-width scatter of 6°. It can be observed that the discretisation with only 16 crystals and the von Mises model as the isotropic background corresponds well to the measured texture. The model is able to reproduce the orientation of the dominant component. However, the intensity of the texture is overestimated. This is a typical behaviour of a Taylor-type model.

The results of the springback measurement and simulation are given in Fig. 3-4. The measurement shows a reduction of the diameter of the lowest ring (4) after the opening. All other rings have an increasing diameter, with the maximum value at the second highest ring (2).

The crystal plasticity models with 7 integration points in thickness direction are in good correlation with the measurements. The diameter reduction of the lowest ring is predicted well. In contrast, the Barlat model with the exponent of m = 2 fails to predict this behaviour. All simulations with the Barlat model and the hybrid model predict the maximum diameter at the highest ring (1), but the differences between ring 1 and 2 are minor if a crystal plasticity model.

**Discussion.** The evaluation of the model behaviour during a deep drawing process and a subsequent cutting and springback operation shows that the number of crystals has only a minor influence on the simulation accuracy. The results of the strain distribution are nearly equal for all configurations under consideration. The application of the crystal plasticity model slightly improves the accuracy of the strain prediction compared to the Barlat model.

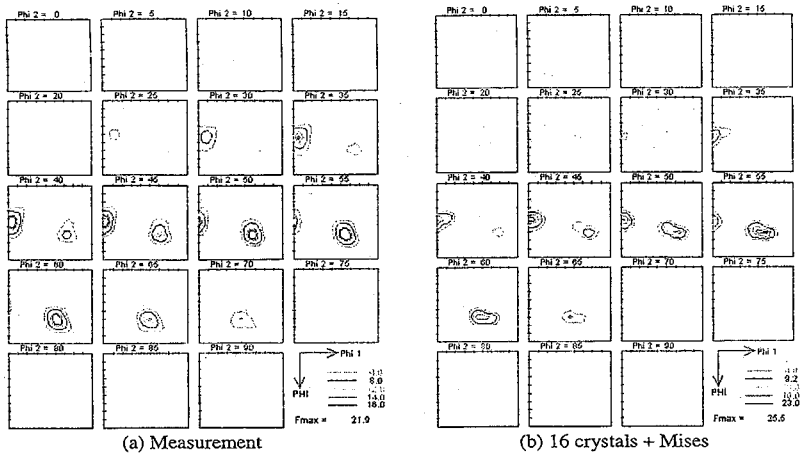


**Fig. 5.** Textures after the deep drawing in rolling direction, measurement and 16-48 crystals with von Mises background

A more interesting result is gained from the earing evaluation. There, the crystal plasticity model with the von Mises background model is able to improve the predictions significantly up to the value of the measurement errors.

The evaluation of the texture development shows that the initial fibre evolves during the deep drawing process into a structure that is dominated by a few components.

The simulation is able to reproduce the development of the primary components of the texture. The orientation of these components is reproduced well, while the intensity of the texture is overestimated, which is a typical behaviour of a Taylor-type model. Considering the springback results, it can be stated that the crystal plasticity



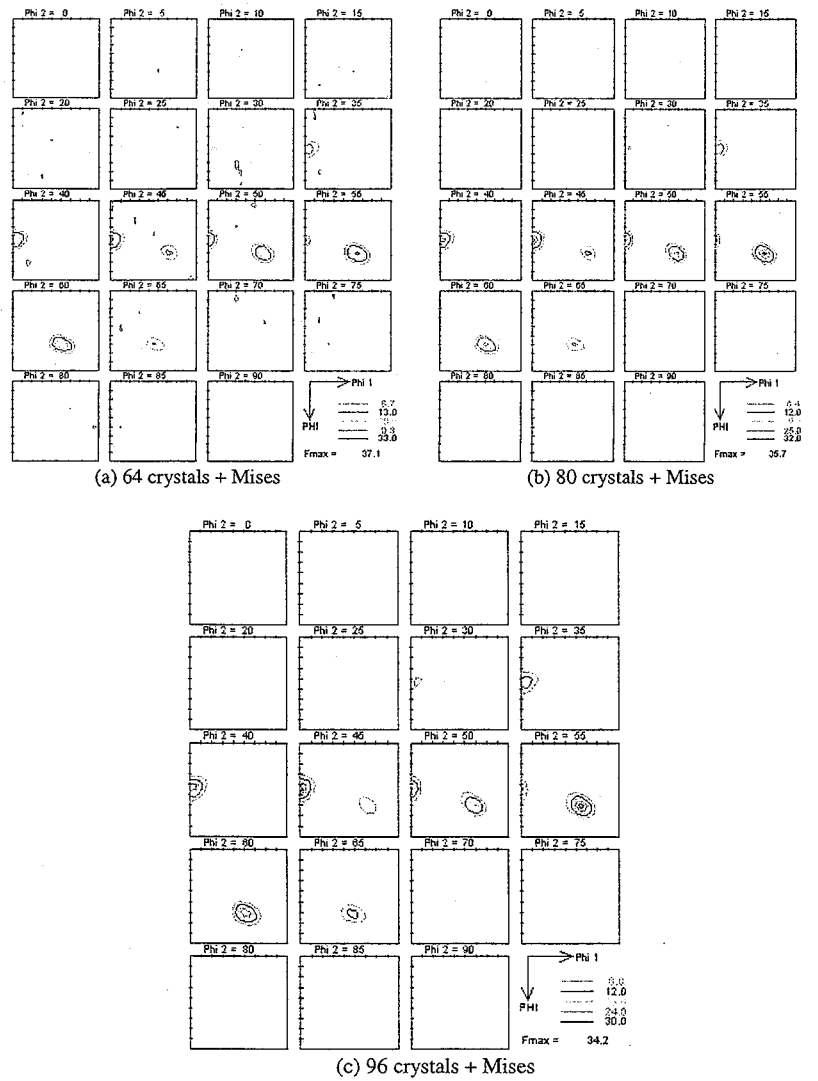


**Fig. 6.** Textures after the deep drawing in rolling direction, 64-96 crystals with von Mises background

model is able to correctly reproduce the qualitative development of the springback. While the Barlat model with m = 2 does not predict the closing of the lowest ring. In other studies (Schulze 2006; Schulze et al. 2007) it is shown that the closing predicted by the Barlat model with m = 6 is also predicted for other materials, that open the

lowest ring. Only the new material model is able to predict this material dependent behaviour correctly.

The overall error of the conventional model is also higher than the one of the crystal plasticity model. The number of crystals does not have a significant impact on the simulation accuracy. Even with only 16 crystals, the qualitative agreement of the numerical predictions is acceptable. Taking all these results into consideration, the crystal plasticity model is able to improve the simulation accuracy for the given case with only 32 crystals and the von Mises component for the approximation of the isotropic background.

## 5 Summary and Conclusions

The study shows how crystallographic information can be incorporated into a continuum mechanical modelling of sheet metal forming. Based on a specific optimisation scheme, a low-dimensional description of the texture is obtained. The model is able to increase the simulation accuracy for a typical deep drawing process with a subsequent springback evaluation. The predictions for the earing profile, the strain distribution in the sheet, and the texture evolution during the deep drawing process are in good agreement with the measurements, if at least 32 crystals are used. For the model identification, a texture measurement is needed in addition to the conventional tension tests in three directions of the blank. Therefore, the measurement effort is not increased dramatically. Even with such a reduced modelling, the computational effort compared with the Barlat model is increased by two orders of magnitude. Therefore, such a model will be available in the near future only with parallel computing as well as for mid size problems.

## References

Barlat, F., Lian, J.: Plastic behavior and stretchability of sheet metals. Part I: A yield function for orthotropic sheets under plane stress conditions. Int. J. Plast. 5, 51–66 (1989)

Barlat, F., Aretz, H., Yoon, J.W., Karabin, M.E., Brem, J.C., Dick, R.E.: Linear transformation-based anisotropic yield functions. Int. J. Plast. 21, 1009–1039 (2005)

Bertram, A.: An alternative approach to finite plasticity based on material isomorphisms. Int. J. Plast. 15(3), 353–374 (1999)

Bertram, A.: Elasticity and Plasticity of Large Deformations. Springer, Heidelberg (2005, 2nd ed (2008)

Böhlke, T.: Crystallographic texture evolution and anisotropy. Simulation, modeling, and applications. Shaker (2001)

Böhlke, T., Haus, U.-U., Schulze, V.: Crystallographic texture approximation by quadratic programming. Acta Mat. 54, 1359–1368 (2006a)

Böhlke, T., Risy, G., Bertram, A.: Finite element simulation of metal forming operations with texture based material models. Modelling Simul. Mater. Sci. Eng. 14, 365–387 (2006b)

Böhlke, T., Glüge, R., Klöden, R., Skrotzki, W., Bertram, A.: Finite element simulation of texture evolution and Swift effect in NiAl under torsion. Modelling Simul. Mater. Sci. Eng. 15, 619–637 (2007)



Böhlke, T., Risy, G., Bertram, A.: micro-mechanically based quadratic yield condition for textured polycrystals. ZAMM 88(5), 379–387 (2008)

Bronkhorst, C.A., Kalidini, S.R., Anand, L.: Polycristalline plasticity and the evolution of crystallographic texture in FCC metals. Philosophical Transactions of the Royal Society London A 341, 443–477 (1992)

Hallquist, J.O.: LS-DYNA theoretical manual. LSTC (1998)

Hill, R.: A theory of the yielding and plastic flow of anisotropic metals. Proc. Roy. Soc. London A 193, 281–297 (1948)

Honneff, H., Mecking, H.: A method for the determination of the active slip systems and orientation changes during single crystal deformation. In: Proceedings of the 5th Conference on Textured Materials (ICOTOM), vol.1, pp. 265–275 (1978)

Krawietz, A.: Materialtheorie. Springer, Heidelberg (1986)

Kröner, E.: Zur plastischen Verformung des Vielkristalls. Acta Metallurgica 9, 155–161 (1961)

Risy, G.: Modellierung der texturinduzierten plastischen Anisotropie auf verschiedenen Skalen. Dissertation, Universität Magdeburg (2006)

Rohleder, M.: Simulation rückfederungsbedingter Formabweichungen im Produktentstehungsprozeß von Blechformteilen. Shaker (2002)

Schulze, V.: Anwendung eines kristallplastischen Materialmodells in der Umformsimulation. Dissertation, Universität Magdeburg (2006)

Schulze, V., Bertram, A., Böhlke, T., Krawietz, A.: Texture-Based Modeling of Sheet Metal Forming and Springback. Preprint 3-2007, Continuum Mechanics, Institute of Engineering Mechanics, Karlsruhe Institute of Technology (2007)

Taylor, G.I.: Plastic strain in metals. J. Inst. Metals 62, 307–324 (1938)

Toth, L., Van Houtte, P.: Discretization techniques for orientation distribution functions. Text. Microstruct. 19, 229–244 (1992)

Albrecht Bertram
Jürgen Tomas

# Micro-Macro-Interactions

## In Structured Media and Particle Systems

Springer